

Shape-Selective Discrimination of Small Organic Molecules

Avijit Sen and Kenneth S. Suslick*

School of Chemical Sciences
University of Illinois at Urbana-Champaign
601 South Goodwin Avenue, Urbana, Illinois 61801

Received January 3, 2000
Revised Manuscript Received October 3, 2000

Over the past few decades there has been remarkable progress in the synthesis of molecular scaffolds based on superstructured porphyrins.¹ A number of these modified porphyrins have been synthesized to mimic various aspects of the enzymatic functions of heme proteins, especially oxygen binding (myoglobin and hemoglobin), and substrate oxidation (cytochrome P-450).^{1,2} The notable property of many heme proteins is their remarkable substrate selectivity; the development of highly regioselective synthetic catalysts, however, is still at an early stage. Discrimination of one site on a molecule from another and distinguishing among many similar molecules presents a difficult and important challenge to both industrial and biological chemistry.³ Although the axial ligation properties of simple synthetic metalloporphyrins are well documented in literature,⁴ size and shape control of ligation to peripherally modified metalloporphyrins has been largely unexplored, with few notable exceptions, where only limited selectivities have been observed.⁵

We report here the synthesis, characterization, and remarkable shape-selective ligation of silyl ether–metalloporphyrin scaffolds derived from the reaction of 5,10,15,20-tetrakis(2',6'-dihydroxyphenyl)porphyrinatozinc(II) with *tert*-butyldimethylsilyl chloride, whereby the two faces of the Zn(II) porphyrin were protected with six, seven, or eight siloxyl groups. This results in a set of three porphyrins of nearly similar electronics but with different steric encumbrance around the central metal atom present in the porphyrin. Ligation to Zn by classes of different sized ligands reveals shape selectivities as large as 10⁷.

A family of siloxyl-substituted bis-pocket porphyrins were prepared according to the process in Scheme 1.⁶ Zn[(OH)₆PP] and Zn[(OH)₈PP] were obtained^{5a} from demethylation⁷ of corresponding free base methoxy compounds followed by zinc(II) insertion. The methoxy porphyrins were synthesized by acid catalyzed condensation of pyrrole with respective benzaldehydes following Lindsey procedures.⁸ Metalation was done in methanol with Zn(O₂CCH₃)₂. The *tert*-butyldimethylsilyl groups were incorporated into the metalloporphyrin by stirring a DMF solution of hydroxyporphyrin complex with TBDMSiCl in the presence of imidazole.⁹ The octa (Zn(Si₈PP)), hepta (Zn(Si₇OHPP)), and hexa (Zn(Si₆PP)) silyl ether porphyrins were obtained from Zn-[(OH)₈PP] and Zn[(OH)₆PP], respectively. The compounds were purified by silica gel column chromatography and fully characterized by UV–visible, ¹H NMR, HPLC, and MALDI-TOF MS.

(1) (a) Suslick, K. S.; Reinert, T. J. *J. Chem. Ed.* **1985**, 62, 974. (b) Collman, J. P.; Zhang, X.; Lee, V. J.; Uffelman, E. S.; Brauman, J. I. *Science* **1993**, 261, 1404.

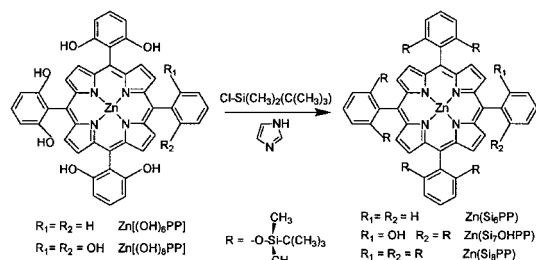
(2) (a) Collman, J. P.; Zhang, X. In *Comprehensive Supramolecular Chemistry*; Atwood, J. L., Davies, J. E. D., MacNicol, D. D., Vogtel, F., Eds.; Pergamon: New York, 1996; Vol. 5, pp 1–32. (b) Suslick, K. S.; van Deusen-Jeffries, S. In *Comprehensive Supramolecular Chemistry*; Atwood, J. L., Davies, J. E. D., MacNicol, D. D., Vogtel, F., Eds.; Pergamon: New York, 1996; Vol. 5, pp 141–170. (c) Suslick, K. S. In *Activation and Functionalization of Alkanes*; Hill, C. L., Ed.; Wiley & Sons: New York, 1989; pp 219–241.

(3) *Metalloporphyrins in Catalytic Oxidations*; Sheldon, R. A., Ed.; Marcel Dekker: New York, 1994.

(4) (a) Bampos, N.; Marvaud, V.; Sanders, J. K. M. *Chem. Eur. J.* **1998**, 4, 325. (b) Stibrany, R. T.; Vasudevan, J.; Knapp, S.; Potenza, J. A.; Emge, T.; Schugar, H. J. *J. Am. Chem. Soc.* **1996**, 118, 3980.

(5) (a) Bhyrappa, P.; Vaijayanthimala, G.; Suslick, K. S. *J. Am. Chem. Soc.* **1999**, 121, 262. (b) Imai, H.; Nakagawa, S.; Kyuno, E. *J. Am. Chem. Soc.* **1992**, 114, 6719.

Scheme 1



The size and shape selectivities of the binding sites of these bis-pocket Zn silyl ether porphyrins were probed using the axial ligation of various nitrogenous bases of different shapes and sizes in toluene at 25 °C. Zn(II) porphyrins were chosen for this study because, in solution, they generally bind only a single axial ligand. Successive addition of ligand to the porphyrin solutions caused a red-shift of the Soret band typical of coordination to zinc porphyrin complexes. There is no evidence from the electronic spectra of these porphyrins for significant distortions of the electronic structure of the porphyrin. The binding constants (K_{eq}) and binding composition (always 1:1) were evaluated using standard procedures.¹⁰ The K_{eq} values of the silyl ether porphyrins with nitrogenous bases of different classes are compared with the sterically undemanding Zn(TPP) in Figure 1. It is worth noting the parallel between shape selectivity in these equilibrium measurements and prior kinetically controlled epoxidation and hydroxylation.^{2,11} While direct comparisons are not yet available, the selectivity for equilibrated ligation appears to be substantially larger than that for irreversible oxidations of similarly shaped substrates.

The binding constants of silyl ether porphyrins are remarkably sensitive to the shape and size of the substrates relative to Zn(TPP) (Figure 1). The binding constants of different amines could be controlled over a range of 10¹ to 10⁷ relative to Zn(TPP). We believe that these selectivities originate from strong steric repulsions created by the methyl groups of the *tert*-butyldimethylsilyloxy substituents. The steric congestion caused by these bulky silyl ether groups is pronounced *even* for linear amines and small cyclic amines (e.g., azetidine and pyrrolidine).

There are very large differences in K_{eq} for porphyrins having three versus four silyl ether groups on each face (e.g., hexa- vs

(6) (a) Abbreviations: Zn(TPP), 5,10,15,20-tetraphenylporphyrinatozinc(II); Zn[(OH)₆PP], 5-phenyl-10,15,20-tris(2',6'-dihydroxyphenyl)porphyrinatozinc(II); Zn[(OH)₈PP], 5,10,15,20-tetrakis(2',6'-dihydroxyphenyl)porphyrinatozinc(II); Zn(Si₆PP), 5-phenyl-10,15,20-tris(2',6'-disilyloxyphenyl)porphyrinatozinc(II); Zn(Si₇OHPP), 5,10,15-tris(2',6'-disilyloxyphenyl)-20-(2'-hydroxy-6'-silyloxyphenyl)porphyrinatozinc(II); Zn(Si₈PP), 5,10,15,20-tetrakis(2',6'-disilyloxyphenyl)porphyrinatozinc(II); TBDMSiCl, *tert*-butyldimethylsilyl chloride. (b) Characterization details provided as Supporting Information. (c) X-ray structure of Zn(Si₈PP) determined at 173(2) K from single crystals grown from a mixture of CHCl₃ and C₆H₆Cl (3:1, v/v). X-ray data collected with a Bruker SMART system with a CCD detector; λ (Mo K α) = 0.7107 Å. Structure solved by direct methods (G. M. Sheldrick, 1998, SHELX-97-2; Institute for Anorg. Chemie, Göttingen, Germany) and refined by full-matrix least squares against all F^2 data. Crystal data for Zn(Si₈PP): crystal dimension 0.20 × 0.22 × 0.24 mm, triclinic, space group $P1$, $a = 13.114(3)$ Å, $b = 13.577(3)$ Å, $c = 28.590(6)$ Å, $\alpha = 78.703(8)^\circ$, $\beta = 83.449(8)^\circ$, $\gamma = 89.214(8)^\circ$, $V = 4959(2)$ Å³, $Z = 2$, $2\theta_{max} = 50^\circ$, $R_1 = 0.0793$, $wR_2 = 0.1944$ (due to some disorder of one of the *t*-Bu groups), GOF = 1.018, residual electron density $-0.417(0.671)$ eÅ⁻³. Details provided as Supporting Information.

(7) Momenteau, M.; Mispelter, J.; Loock, B.; Bisagni, E. *J. Chem. Soc., Perkin Trans. 1* **1983**, 189.

(8) Lindsey, J. S.; Wagner, R. W. *J. Org. Chem.* **1989**, 54, 828.

(9) Corey, E. J.; Venkateswarlu, A. *J. Am. Chem. Soc.* **1972**, 94, 6190.

(10) (a) Collman, J. P.; Brauman, J. I.; Doxsee, K. M.; Halbert, T. R.; Hayes, S. E.; Suslick, K. S. *J. Am. Chem. Soc.* **1978**, 100, 2761. (b) Suslick, K. S.; Fox, M. M.; Reinert, T. *J. Am. Chem. Soc.* **1984**, 106, 4522.

(11) (a) Bhyrappa, P.; Young, J. K.; Moore, J. S.; Suslick, K. S. *J. Am. Chem. Soc.* **1996**, 118, 5708–5711. (b) Suslick, K. S.; Cook, B. R. *J. Chem. Soc., Chem. Commun.* **1987**, 200–202. (c) Cook, B. R.; Reinert, T. J.; Suslick, K. S. *J. Am. Chem. Soc.* **1986**, 108, 7281–7286. (d) Suslick, K. S.; Cook, B. R.; Fox, M. M. *J. Chem. Soc., Chem. Commun.* **1985**, 580–582.

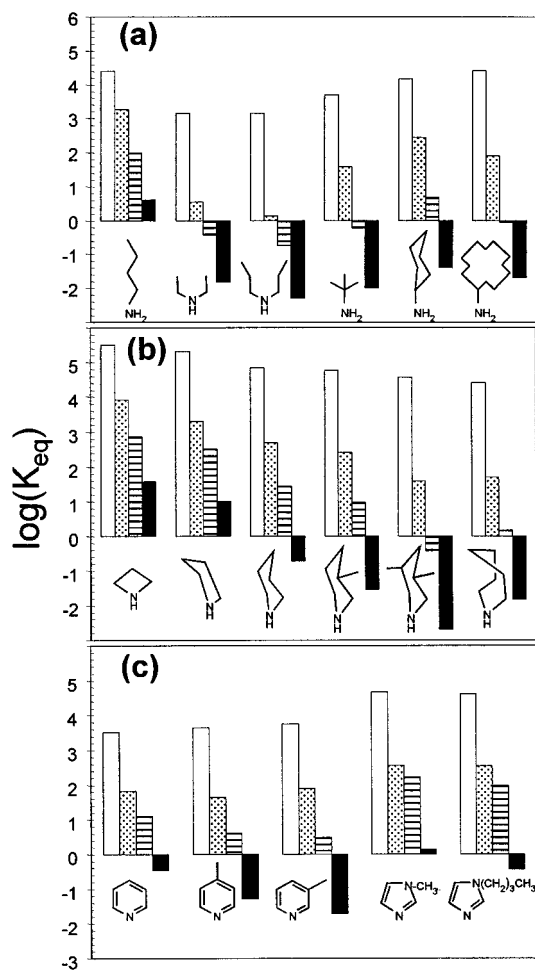


Figure 1. Ligand binding constants for siloxyl porphyrins compared to Zn(TPP): (a) aliphatic primary and secondary amines; (b) alicyclic secondary amines, and (c) aromatic amines. Errors in K_{eq} were typically $\pm 10\%$ (i.e., ± 0.05 log units): open bar, Zn(TPP); dotted bar, Zn(Si₆-PP); horizontally ruled bar, Zn(Si₇-OHPP); and solid bar, Zn(Si₈-PP).

octasilyl ether porphyrins), as expected based on obvious steric arguments (Figure 1). Even between the hexa- over heptasilyl ether porphyrins, however, there are still substantial differences in binding behavior. We suggest that this is probably due to doming of the macrocycle in the hexa- and heptasilyl ether porphyrins, which lessens the steric constraint relative to the octasilyl ether porphyrin. Such doming will be especially important in porphyrins whose two faces are not identical. The free hydroxy functionality of the heptasilyl ether may play a role in binding of bifunctionalized ligands (e.g., free amino acids); for the simple amines presented here, however, we have no evidence of any special effects.

These silyl ether porphyrins showed remarkable selectivities for *normal*, linear amines over their cyclic analogues. For a series of linear amines (*n*-propylamine through *n*-decylamine), K_{eq} values were very similar for each of the silyl ether porphyrins. In comparison, the relative K_{eq} for linear versus cyclic primary amines (Figure 1a, *n*-butylamine vs cyclohexylamine) were significantly different: $K_{eq}^{linear}/K_{eq}^{cyclic}$ ranges from 1 to 23 to 115 to >200 for Zn(TPP), Zn(Si₆-PP), Zn(Si₇-OHPP), and Zn(Si₈-PP), respectively. The ability to discriminate between linear and cyclic compounds is thus established.

A series of cyclic secondary amines (Figure 1b) demonstrate the remarkable size and shape selectivities of this family of bis-pocket porphyrins, whereas the binding constants to Zn(TPP) with those amines are virtually similar. In contrast, the K_{eq} values for silyl ether porphyrins strongly depend on the ring size and its peripheral substituents. The effect of these shape-selective binding

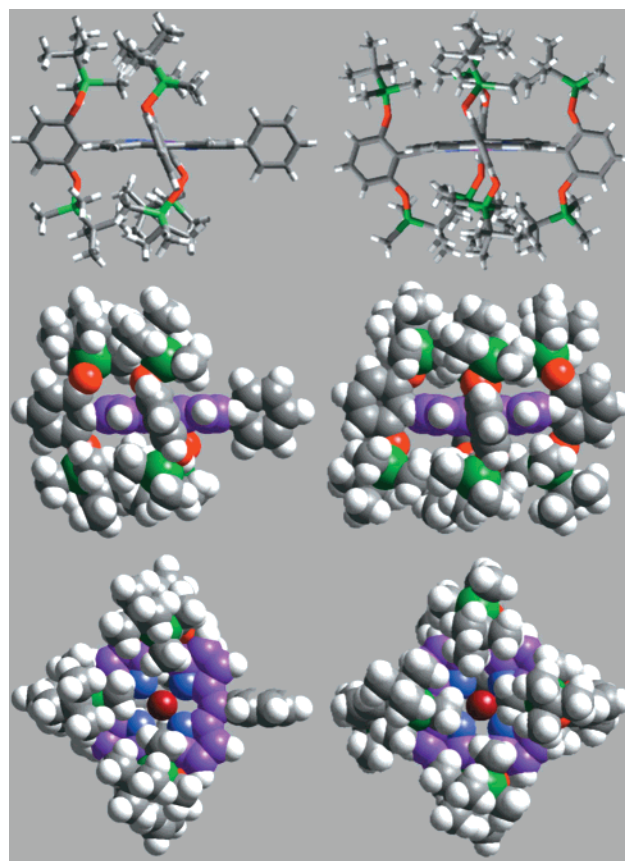


Figure 2. Molecular models of Zn(Si₆-PP) (left column) and Zn(Si₈-PP) (right column). Pairs of images (top to bottom) are cylinder side-views, side-views, and top-views, respectively; space filling shown at 70% van der Waals radii, with porphyrin carbon atoms (purple), oxygen atoms (red), silicon atoms (green), and Zn (dark red). The X-ray single-crystal structure of Zn(Si₈-PP) determined at 173(2) K is shown;^{6c} for Zn(Si₆-PP), an energy-minimized structure was obtained using Cerius 2 from MSI.

sites is clear, even for compact aromatic ligands with non-*ortho*-methyl substituents (Figure 1c).

The molecular structures of these silyl ether porphyrins explain their ligation selectivity. We have solved the X-ray single-crystal structure of Zn(Si₈-PP) in the triclinic *P*1 space group.^{6c} As shown in Figure 2, Zn(Si₆-PP) (energy minimized molecular model) and Zn(Si₈-PP) (single crystal X-ray structure) have dramatically different binding pockets. In the octasilyl ether porphyrin, the top access on both faces of the porphyrin is very tightly controlled by the siloxyl pocket. In contrast, the metal center of the hexasilyl ether porphyrin is considerably more exposed for ligation.

In summary, a series of bis-pocket siloxylmetalloporphyrin complexes were prepared with sterically restrictive binding pockets on both faces of the macrocycle. Ligation to Zn by various nitrogenous bases of different sizes and shapes was investigated. Shape selectivities as large as 10^7 were found, compared to unhindered metalloporphyrins. Fine-tuning of ligation properties of these porphyrins was also possible using pockets of varying steric demands. The shape selectivities shown here rival or surpass those of any biological system.

Acknowledgment. We thank Dr. Richard Milberg (UIUC, Mass Spectroscopy Lab) for MALDI-TOF spectral measurements and Drs. J. H. Chou and S. R. Wilson for assistance in solving the crystal structure. This work was supported by the National Institute of Health (HL 5R01-25934) and in part by the U.S. Army Research Office (DAAG55-97-0126).

Supporting Information Available: Synthesis, characterization, and X-ray crystallographic details (PDF). This material is available free of charge via the Internet at <http://pubs.acs.org>.

JA000002J